From Quasiperiodicity to a Complete Coloring of the Kohmoto Butterfly

Ram Band[1] and Siegfried Beckus[2]

[1]*Department of Mathematics, Technion–Israel Institute of Technology, Haifa, Israel*

[2]*Institute of Mathematics, University of Potsdam, Potsdam, Germany*

The spectra of the Kohmoto model give rise to a fractal phase diagram, known as the Kohmoto butterfly. The butterfly encapsulates the spectra of all periodic Kohmoto Hamiltonians, whose index invariants are sought after. Topological methods – such as Chern numbers – are ill defined due to the discontinuous potential, and hence fail to provide index invariants. This Letter overcomes that obstacle and provides a complete classification of the Kohmoto model indices. Our approach encodes the Kohmoto butterfly as a spectral tree graph, reflecting the quasiperiodic nature via the periodic spectra. This yields a complete coloring of the phase diagram and a new perspective on other spectral butterflies.

Quasicrystals exhibit challenging spectral and topological properties. Their quasiperiodic order gives rise to fractal spectra with infinitely many spectral gaps, manifest in diverse wave systems [1–3].

Topology together with a variety of mathematical methods enables a classification of quasicrystals into equivalence classes governed by topological invariants [4–7]. Beyond the mathematical aspects, a wide range of phenomena arise and are studied across theoretical and experimental physics as well as engineering [8–13]. Nevertheless, there are topological shortcomings when trying to study Kohmoto model [14], a paradigmatic model of quasicrystals. The three main approaches towards topological indices are not applicable to the Kohmoto model: Chern numbers rely on differentiability of the spectral projections [5], and so are not defined; the bulk–boundary correspondence (Thouless pump [15, 16]) breaks down; and the two-dimensional extension (via inverse Fourier transform) gives a parent Hamiltonian with a nonlocal slowly decaying potential, hence not possessing a Fredholm index [17]. This Letter overcomes these obstacles and presents an approach that yields natural indices for the Kohmoto model. These indices consistently reflect the quasiperiodic limit, allow to color the corresponding phase diagram (Kohmoto butterfly) and suggest new physical invariants.

The Kohmoto model [14] is given by the Hamiltonians

$$(H_\alpha\psi)(n) = \psi(n+1) + \psi(n-1) + V_\alpha(n)\,\psi(n), \qquad (1)$$

where the potential $V_\alpha(n) = \lambda\chi_{[1-\alpha,1)}(n\alpha \mod 1)$ is determined by a frequency α, a coupling constant (a.k.a modulation amplitude) λ and $\chi_{[1-\alpha,1)}$ is the characteristic function of the interval $[1-\alpha, 1)$. It is well-known that these quasiperiodic operators represent one-dimensional quasicrystals. For instance, the Fibonacci quasicrystal $\alpha = \frac{\sqrt{5}-1}{2}$ forms a prominent and well-studied example in this class [18, 19].

For rational frequencies $\alpha = \frac{p}{q}$, the operator $H_{\frac{p}{q}}$ is q-periodic and its spectrum consists of q spectral bands. The integrated density of states (IDS), a.k.a. electron density, is

$$N_\alpha(E) = \frac{n}{q} = \mathfrak{c}\alpha \mod 1 \qquad (2)$$

for energies E in the n-th gap. The index $\mathfrak{c}$ solving the Diophantine equation above is defined only modulo q. The same Diophantine equation appears in the Hofstadter model [20, 21] of the quantum Hall effect. In that case, the modulo q ambiguity is resolved by identifying $\mathfrak{c}$ with a Chern number, which can be computed from the Berry's curvature of the corresponding spectral projection [22, 23]. This endows $\mathfrak{c}$ with topological significance, as Chern numbers are invariant under variations that do not close the spectral gap. When one assigns a color to each integer value, this provides a consistent coloring of the phase diagram (Hofstadter butterfly) [24, 25].

In the Kohmoto model $\mathfrak{c}$ cannot be identified with a Chern number, since the potential V_α is discontinuous, and Berry's phase needs the spectral projections to be differentiable [26]. Therefore, a coloring of the Kohmoto butterfly is not possible without further insights for resolving the modulo q ambiguity inherent in (2); see [27].

We provide here a consistent coloring (depicted in Fig. 1, Left) by resolving this ambiguity and determining the values of the index invariants. We start by presenting the connection between the periodic Hamiltonians (with $\alpha \in \mathbb{Q}$) and the quasiperiodic ones ($\alpha \notin \mathbb{Q}$), where the former may be used to approximate the latter.

Let $\alpha \notin \mathbb{Q}$ be written in terms of its continued fraction expansion,

$$\alpha = a_0 + \cfrac{1}{a_1 + \cfrac{1}{a_2 + \cfrac{1}{\ddots}}}, \qquad (3)$$

where $a_0 = 0$ and $a_n \in \mathbb{N}$ for all $n \in \mathbb{N}$. Truncating this expansion gives finite continued fraction expansions,

$$\alpha_k = a_0 + \cfrac{1}{a_1 + \cfrac{1}{\ddots + \frac{1}{a_k}}} = \frac{p_k}{q_k}, \qquad k \in \mathbb{N}\cup\{0\}, \qquad (4)$$

where $p_k, q_k \in \mathbb{N}$ are chosen to be coprime. By convention, $\alpha_0 = \frac{p_0}{q_0} = \frac{0}{1}$ (as $a_0 = 0$).

We construct an infinite directed tree graph $\mathcal{T}_\alpha$, and name it the spectral α-tree. This tree encodes the periodic approximations H_{α_k} of H_α. Specifically, for each k the vertices at level k represent the spectral bands and gaps of H_{α_k}. The tree is constructed recursively via the digits $\{a_1, a_2, a_3, \ldots\}$ of the continued fraction of α, as illustrated in Fig. 2 and explained next (see also [28, 29]).

We start by fixing a single vertex to be the root of the tree. We say that the root belongs to level $k = -1$ of the tree.

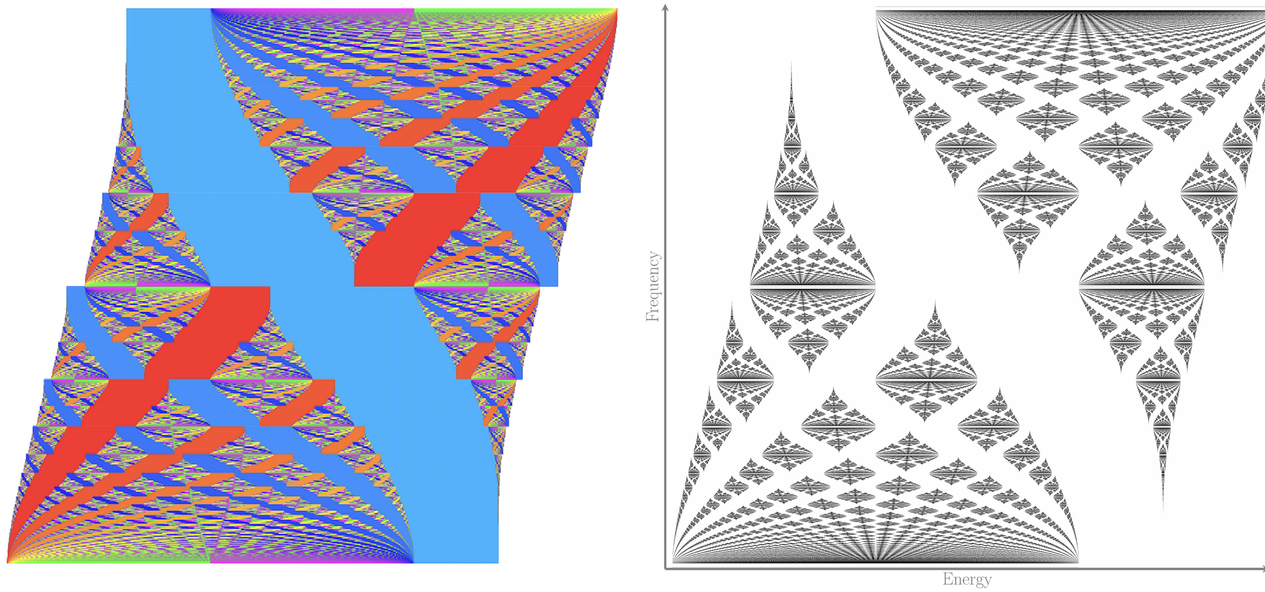

Figure 1. The right panel shows the Kohmoto butterfly – the spectral bands are plotted for different rational frequencies α. In the left panel each spectral gap for a periodic Hamiltonian is colored according to its index.

Starting from the root, all other vertices belong to ascending levels k in the tree and they carry one of the three labels: A, B or G. The label tells whether the vertex represents a spectral gap (label G, appearing as a circle in Fig. 2) or a spectral band (labels A, B). The root is connected to two vertices at level $k=0$, the left has label A and the right has label G. The rest of the tree $\mathcal{T}_\alpha$ is constructed recursively: for every vertex v with label A or B in level $k \geq 0$, denote

$$M := \begin{cases} a_{k+1}-1, & \text{if } v \text{ has the label } A, \\ a_{k+1}, & \text{if } v \text{ has the label } B, \end{cases} \tag{5}$$

and connect the vertex v to $2M+1$ vertices in level $k+1$. The labels of these vertices alternate between G and A, starting and ending with G, see Fig. 2. For a G-vertex v in level k, connect it to a single B-vertex in level $k+1$. This provides a complete description of $\mathcal{T}_\alpha$ [30].

Each vertex of the tree represents a spectral band or spectral gap of H_{α_k} as shown in Fig. 2. The ordering of the vertices within a certain level k corresponds to the spectral order [29]. In addition, if two vertices of spectral bands (i.e., of labels A/B) are connected by a directed path, it means that the upper band is fully contained in the lower as is demonstrated in Fig. 2.

We now use the tree $\mathcal{T}_\alpha$ to assign indices to the spectral gaps (i.e., to the G-vertices). For each level k, count the number of A-vertices at level k and denote this number by $Z_A(k)$. Similarly, denote the number of B-vertices in level k by $Z_A(k)$. For each G-vertex v in level k, count how many A and B vertices there are at level k to the left of v and denote these numbers by $z_A(v)$ and $z_B(v)$. Combine this information to form the matrix:

$$Q_k(v) = \begin{pmatrix} Z_A(k) & z_A(v) \\ Z_A(k) & z_B(v) \end{pmatrix}. \tag{6}$$

See Fig. 3 for examples of $Q_k(v)$ for two vertices. Using this matrix we assign the following index to the spectral gap represented by v:

$$\mathfrak{c}_k(v) = (-1)^k \det Q_k(v) \, mod^* \, q_k. \tag{7}$$

The notation mod^* stands for the centered modulo (a.k.a. symmetric modulo) which is defined as

$$x \, mod^* \, q := x - q \left\lfloor \frac{x}{q} + \frac{1}{2} \right\rfloor \in \left[-\frac{q}{2}, \frac{q}{2}\right) \cap \mathbb{Z}, \tag{8}$$

where $\lfloor \cdot \rfloor$ is the floor function. Note that we have slightly changed here the conventional definition of mod^*, by including $-\frac{q}{2}$, rather than $\frac{q}{2}$, as is usually done. See the supplementary material, Sec. E for an explanation of the rationale behind this choice. Fig. 3 demonstrates the $\mathfrak{c}_k(v)$ values which are assigned to vertices in the few first levels of a particular tree $\mathcal{T}_\alpha$.

First, note that the index $\mathfrak{c}_k(v)$ in (7) is indeed a solution for the Diophantine equation (2), see supplementary material, Sec. A. We proceed to further demonstrate that $\mathfrak{c}_k(v)$ is actually the natural solution for the modulo q ambiguity when taking into account the governing quasiperiodic structure.

Fix a rational number $\frac{p}{q} \in \mathbb{Q}$. Take a spectral gap of $H_{\frac{p}{q}}$ to which one wants to assign an index. Choose a finite continued fraction which represents $\frac{p}{q}$ as in (4). Extend it arbitrarily to obtain an irrational $\alpha \notin \mathbb{Q}$. This means that there is a $k \in \mathbb{N}_0$ such that $\frac{p}{q} = \alpha_k$, so $\frac{p}{q}$ is a rational approximation of α. Now, consider the tree $\mathcal{T}_\alpha$ and let v be the vertex representing the chosen spectral gap of $H_{\frac{p}{q}}$. This G-vertex v with index $\mathfrak{c}_k(v)$ can be seen as an approximation of a particular gap of the quasiperiodic Hamiltonian H_α, as is explained below. This spectral gap of H_α has a well-defined (i.e., non-ambiguous) index $\mathfrak{c} \in \mathbb{Z}$, such that the IDS satisfies

$$N_\alpha(E) = \mathfrak{c}\alpha \mod 1, \qquad \mathfrak{c} \in \mathbb{Z}, \tag{9}$$

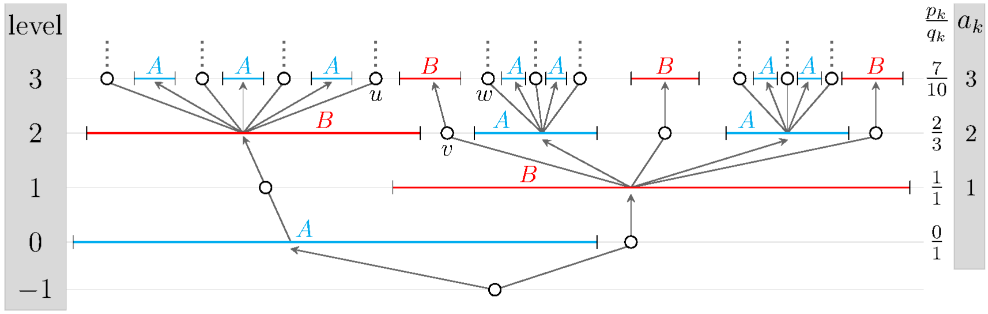

Figure 2. An example of a spectral α-tree is sketched if α has continued fraction expansion $(a_k)_{k=0}^{\infty}$ starting with $0, 1, 2, 3$. The vertices of the graph are drawn as the spectral bands to which they correspond; their labels (A/B) are indicated. Vertices representing gaps G are indicated by circles.

for energies E in that gap. This results from the gap labelling theorem [31]. Note that (9) has the same form as (2), however, it does not carry the same modulu ambiguity, since here α is irrational. This substantial difference is a key ingredient in the ambiguity resolution. We proceed to show that the index of the gap of $H_{\frac{p}{q}}$ coincides with the index of the corresponding gap of H_α, i.e., $\mathfrak{c}_k(v) = \mathfrak{c}$. This is independent of how we choose α. Therefore $\mathfrak{c}_k(v)$ reflects the quasiperiodic structure and our index choice resolves the bespoken modulo ambiguity.

To determine the mentioned spectral gap in H_α, we construct (sketched in Fig. 3) an infinite path γ in the tree $\mathcal{T}_\alpha$ starting from v, such that all the G vertices of γ have the index $\mathfrak{c} = \mathfrak{c}_k(v)$ as well.

The construction depends on the sign of $\mathfrak{c}_k(v)$ and the parity of k. Assume first that either ***(i)*** k is even and $\mathfrak{c}_k(v)$ is positive, or ***(ii)*** k is odd and $\mathfrak{c}_k(v)$ is negative. We set the first vertex of γ to be v; the second vertex is the single B vertex at level $k+1$ which emanates from v. Afterwards in each level $k+m+1$ (for $m \geq 1$), γ is defined by choosing the right-most vertex which emanates from its vertex at level $k+m$. This uniquely determines a path starting at v where the vertex labels alternate between G and B. The complementary scenario is either ***(iii)*** k is even and $\mathfrak{c}_k(v)$ is negative or ***(iv)*** k is odd and $\mathfrak{c}_k(v)$ is positive. Then, we act in a reverse manner: start from v and construct γ by always picking the left-most vertex when branching, see an example in Fig. 3.

We continue to verify that all G-vertices in γ have the same index. Let v be a G-vertex at level k. It is connected to a unique B-vertex at level $k+1$ and its neighboring G-vertices are denoted by u and w (u on the left, w on the right, as exemplified in Fig. 2). The Q matrices of these vertices are related as follows

$$\begin{aligned} Q_{k+1}(w) &= Q_{k+1}(u) + \begin{pmatrix} 0 & 0 \\ 0 & 1 \end{pmatrix} \\ &= T_{k+1} Q_k(v) + \begin{pmatrix} 0 & 0 \\ 0 & k \mod 2 \end{pmatrix}, \end{aligned} \tag{10}$$

where $T_k = \begin{pmatrix} a_k - 1 & a_k \\ 1 & 1 \end{pmatrix}$ with a_k being the digits of the continued fraction expansion of α. Validating (10) is straightforward given the tree branching structure and that in each level we alter between G-vertices and vertices with label A or B. Now, let $\gamma = (v_0, v_1, v_2, \ldots)$ be an infinite path, as described above, starting from $v = v_0$ at level k. Then all the even vertices v_{2m} are G-vertices. Using $\det T_k = -1$ for all k, we conclude $\mathfrak{c}_k(v_0) = \mathfrak{c}_{k+2m}(v_{2m})$ for all $m \in \mathbb{N}$ from (7) and (10). More details are provided in supplementary material, Sec. C.

We proceed to describe the gap of H_α which corresponds to γ and show that its index equals to the common value $\mathfrak{c}_k(v_0) = \mathfrak{c}_{k+2m}(v_{2m})$ of all G-vertices of γ, as mentioned above. The vertices of γ alternate between the labels G and B (the first vertex v_0 has label G). The G-vertices represent spectral gaps of the periodic operators; these spectral gaps converge to a spectral gap of H_α, [32], see Sec. D. Furthermore, the infinite paths γ described above come in pairs, with each path representing one boundary (left/right) of a spectral gap of H_α [29, 33], see Fig. 3. The conservation law holds for all indices $\mathfrak{c}_k$ on both paths.

Pick a spectral gap I of H_α and let $\gamma = (v_0, v_1, v_2, \ldots)$ be the left path whose gaps (represented by the vertices $\{v_{2m}\}$) converge to the chosen gap I of H_α; we choose the left path as an example, but all arguments work as well for the right path with suitable right/left switches. For each $m \geq 0$ denote by E_m the right boundary of the gap represented by v_{2m}. The energies $\{E_m\}$ converge to the right boundary of I (Sec. D), which we denote by E. The IDS values of the periodic operators at these energies satisfy $N_{\alpha_{k+2m}}(E_m) = \mathfrak{c}_{k+2m}(v_{2m})\alpha_k \mod 1$, since the index $\mathfrak{c}_{k+2m}(v_{2m})$ was shown to satisfy the Diophantine equation (2). By the definition of the IDS [29] together with the convergence $E_m \to E$ and $\alpha_{k+2m} \to \alpha$ we get $N_{\alpha_{k+2m}}(E_m) \to N_\alpha(E)$ as $m \to \infty$. The gap labelling theorem [31] yields $N_\alpha(E) = \mathfrak{c}\alpha \mod 1$ for some value $\mathfrak{c} \in \mathbb{Z}$, as in (9). Hence, by the conservation $\mathfrak{c}_k(v_0) = \mathfrak{c}_{k+2m}(v_{2m})$ shown above and the convergence of the IDS values, we get that this conserved index equals the index $\mathfrak{c}$ of the quasiperiodic operator H_α, i.e. $\mathfrak{c}_{k+2m}(v_{2m}) = \mathfrak{c}$ for all $m \geq 0$. This concludes the arguments justifying the Kohmoto model indices.

To summarize, this Letter establishes a full classification of the indices of the Kohmoto model, and while doing so three additional goals are reached. First, the tree-based description

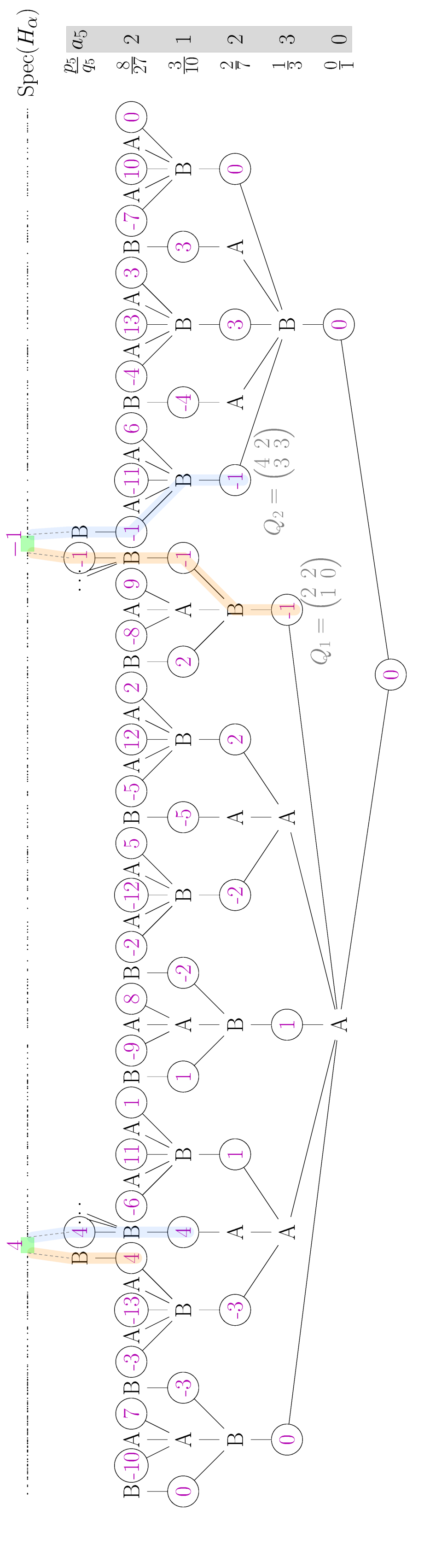

Figure 3. Illustration of the tree for a continued fraction beginning with $0, 3, 2, 1, 2$. The index is marked within the circle of the G-vertex. Four G-vertices are highlighted with the corresponding infinite paths having index $\mathfrak{c}_k(v) = -1$ respectively $\mathfrak{c}_k(v) = 4$.

shows that the spectra of all periodic Kohmoto Hamiltonians are intrinsically connected, collectively forming the Kohmoto butterfly (Fig. 1, Right). Furthermore, it provides a structural framework to investigate related quasiperiodic models and to deepen the understanding of their indices.

Second, the tree structure exposes that the quasiperiodicity is reflected in the periodic approximations. By the recent resolution of the dry ten Martini problem [28, 29] it is known that all integer values show up as an index value in (9). Explicitly, when fixing $\alpha \notin \mathbb{Q}$, we know that every integer value $\mathfrak{c} \in \mathbb{Z}$ appears as the index value of some open gap of H_α. The current Letter identifies the minimal periodic (finite-size) approximations that realize every such possible index, and specifies the energy gaps in which that value occurs. The ability to exactly specify for each index in which finite-size system it appears is substantial for experimental realizations.

Third, for the Kohmoto model we settle the ambiguity problem highlighted in [27] by confirming and sharpening the conjecture posed there. This leads to a full coloring of the topological phase diagram of the Kohmoto model (Fig. 1, Left), in a direct analogy to Hofstadter's colored butterfly [24, 25]. Nevertheless, the two models are substantially different. In contrary to the Hofstadter butterfly, the complement of the Kohmoto butterfly consists of a single connected component. Due to this, the gap indices are not restricted to connected components of the phase diagram (Fig. 1) as opposed to the Hofstadter butterfly. For example, one can see in the colored Kohmoto butterfly that the red phases terminate without a gap continuously shrinking and closing. This is against the folk wisdom, grounded in smooth models. On the other hand, the color ordering in the phase diagram is identical for both butterflies, highlighting a similarity between the two models. This provides another perspective on the question of topological equivalence between the Kohmoto and Hofstadter models; a question raised in [34] and gained a substantial progress in [35, 36], but not yet conclusively resolved.

ACKNOWLEDGMENTS

We are grateful to Joseph Avron, Eric Akkermans, Johannes Kellendonk, Laurent Raymond, Hermann Schulz-Baldes, Jacob Shapiro, Gilad Sofer, Yannik Thomas and Oded Zilberberg for inspiring discussions. The research for this article was partially conducted at the Israel Institute for Advanced Studies, as part of the Research Group Analysis, Geometry, and Spectral Theory of Graphs during 2025.

SUPPLEMENTARY MATERIAL

We add here further details about the calculations included in this work.

A. Deriving Eq. (2)

Consider a rational number $\frac{p}{q}$ and an irrational α such that $\alpha_k = \frac{p}{q}$. Let v be a G-vertex representing a spectral gap of $\mathrm{Spec}\,(H_{\alpha_k})$ with index $\mathfrak{c}_k(v)$. Then v corresponds to the n-th spectral gap in $\mathrm{Spec}\,(H_{\alpha_k})$ with $n = z_A(v) + z_B(v)$ and $N_{\alpha_k}(E) = \frac{n}{q}$.

By the theory of continued fractions, we have $p_k q_{k-1} - p_{k-1} q_k = (-1)^{k-1}$, equivalently, $p_k q_{k-1} = (-1)^{k-1} \mod q_k$. Since $q_{k-1} = Z_A(k-1) + Z_A(k-1) = Z_A(k)$ and $Z_A(k) + Z_A(k) = q_k$ by the basic properties of the tree $\mathcal{T}_\alpha$, we get $p_k Z_A(k) = (-1)^{k-1} \mod q_k$ and $p_k Z_A(k) = (-1)^k \mod q_k$. Denoting $\mathfrak{i}_k(v) := (-1)^k \det Q_k(v)$ this implies

$$\begin{aligned}\mathfrak{i}_k(v) p_k &\equiv (-1)^k \left(Z_A(k) z_B(v) - Z_A(k) z_A(v)\right) p_k \mod q_k \\ &\equiv z_B(v) + z_A(v) \equiv n \mod q_k.\end{aligned}$$

By (7), $\mathfrak{i}_k(v) = \mathfrak{c}_k(v) \mod q_k$ validating the Diophantine equation (2).

We note that the identity $\left(p_k^{-1} \mod q_k\right) = (-1)^{k-1} q_{k-1}$ is a consequence of the above, and it may be used for explicitly solving (2) and coloring the Kohmoto butterfly.

B. Deriving Eq. (10)

Let v be a G-vertex at level k in a spectral α-tree. It is connected to a unique B-vertex v' at level $k+1$, with u and w the neighboring G-vertices. This immediately yields

$$Q_{k+1}(w) = Q_{k+1}(u) + \begin{pmatrix} 0 & 0 \\ 0 & 1 \end{pmatrix}.$$

For the second equality in Eq. (10), start by justifying the left column, i.e.

$$\begin{pmatrix} Z_A(k+1) \\ Z_A(k+1) \end{pmatrix} = T_{k+1} \begin{pmatrix} Z_A(k) \\ Z_A(k) \end{pmatrix}. \tag{11}$$

To see this note that ***(i)*** all A-vertices at level $k+1$ emanate from either A or B vertices at level k, and their count is given by the branching degree (5); and ***(ii)*** there is a bijection between all B-vertices at level $k+1$ and all G-vertices at level k. The number of the latter equals the total number of both A and B vertices in level k. It is left to show

$$\begin{pmatrix} z_A(w) \\ z_B(w) \end{pmatrix} = T_{k+1} \begin{pmatrix} z_A(v) \\ z_B(v) \end{pmatrix} + \begin{pmatrix} 0 \\ k \mod 2 \end{pmatrix}. \tag{12}$$

The arguments are similar to those used for (11). The only difference is that the number of G-vertices to the left of v (and including v) equals the total number of A and B vertices to the left of v, plus $(k \mod 2)$. This correction comes since the left most vertex at odd levels is always a G-vertex.

C. Index conservation

We establish here the index conservation along the paths $\gamma = (v_0, v_1, v_2, \ldots)$, described in the Letter. Explicitly, we show that $\mathfrak{c}_k(v_0) = \mathfrak{c}_{k+2m}(v_{2m})$ for all $m \in \mathbb{N}$. As a by-product, our computations justify the choice of the centered window $\left[-\frac{q}{2}, \frac{q}{2}\right)$ in the definition of $\mathfrak{c}_k$, (7). We start by adopting (as in Sec. A) the notation $\mathfrak{i}_k(v) := (-1)^k \det Q_k(v)$, with which (7) reads $\mathfrak{c}_k(v) = \mathfrak{i}_k(v)\, mod^*\, q_k$.

Let v be a G-vertex at level k in a spectral α-tree. It connects to a unique B-vertex at level $k+1$, with u and w the neighboring G-vertices. We begin by showing the following identities: if k is even, then

$$\mathfrak{i}_k(v) = \mathfrak{i}_{k+1}(w) \quad \text{and} \quad \mathfrak{i}_k(v) - q_k = \mathfrak{i}_{k+1}(u) - q_{k+1}, \tag{13}$$

and if k is odd then

$$\mathfrak{i}_k(v) = \mathfrak{i}_{k+1}(u) \quad \text{and} \quad \mathfrak{i}_k(v) - q_k = \mathfrak{i}_{k+1}(w) - q_{k+1}. \tag{14}$$

Since $\det(T_k) = -1$, $\det\left(T_{k+1} Q_k(v)\right) = -\det\left(Q_k(v)\right)$. Together with (10), this yields $\mathfrak{i}_k(v) = \mathfrak{i}_{k+1}(w)$ when k even, and $\mathfrak{i}_k(v) = \mathfrak{i}_{k+1}(u)$ when k is odd. This proofs the first parts of the equations (13) and (14).

For the second part, we compute

$$\begin{aligned}\mathfrak{i}_k(v) - q_k &= (-1)^k \det\left[Q_k(v) + \begin{pmatrix} 0 & (-1)^k \\ 0 & (-1)^{k+1} \end{pmatrix}\right] \\ &= (-1)^{k+1} \det\left[T_{k+1}\left(Q_k(v) + \begin{pmatrix} 0 & (-1)^k \\ 0 & (-1)^{k+1} \end{pmatrix}\right)\right] \\ &= (-1)^{k+1} \det\left[T_{k+1} Q_k(v) + \begin{pmatrix} 0 & (-1)^{k+1} \\ 0 & 0 \end{pmatrix}\right].\end{aligned}$$

Thus, (10) implies if k is even

$$\begin{aligned}\mathfrak{i}_k(v) - q_k &= (-1) \det\left[Q_{k+1}(u) + \begin{pmatrix} 0 & -1 \\ 0 & 1 \end{pmatrix}\right] \\ &= \mathfrak{i}_{k+1}(u) - q_{k+1}\end{aligned}$$

and if k is odd

$$\begin{aligned}\mathfrak{i}_k(v) - q_k &= \det\left[Q_{k+1}(w) + \begin{pmatrix} 0 & 1 \\ 0 & -1 \end{pmatrix}\right] \\ &= \mathfrak{i}_{k+1}(w) - q_{k+1},\end{aligned}$$

which concludes the verification of (13) and (14)

Equations (13) and (14) show that starting from a vertex v, there is a path along which i_k is conserved and another path along which $i_k - q_k$ is conserved. The left/right orientation of those paths depends on the parity of k (see Fig. 4). Consequently, it is natural to select the conserved quantity (either i_k or $i_k - q_k$) as the gap index, since this value remains invariant.

We proceed by induction to show that

$$i_k(v) \in [0, q_k) \tag{15}$$

for all G-vertices v. For $k = 0$ and $k = 1$ this follows directly from computation.

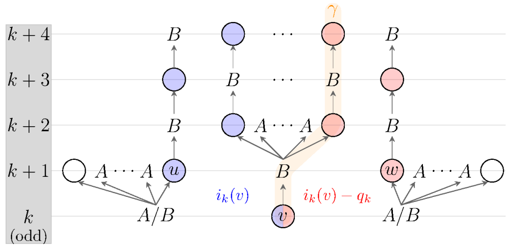

Figure 4. An illustration of the conservation deduced from (13) and (14) for odd k. For all blue vertices $i_*(*)$ is preserved and for all red vertices $i_*(*) - q_*$ is preserved. We indicate the path γ which is the one is chosen if $\mathfrak{c}_k(v) < 0$.

Suppose the claim holds up to level $k-1$, and let v be a G-vertex in level k. If v is a G-vertex with no neighbor on one side (either left or right), then $i_k(v) = 0$ by definition of the matrix $Q_k(v)$. For all other G-vertices, the construction of the spectral tree shows that either v has a neighboring B-vertex or both neighbors are A-vertices, Fig. 5. We treat each of these cases separately.

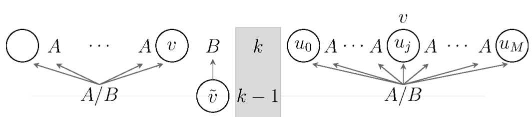

Figure 5. Illustration of different G-vertices: sandwiched between an A-vertex and a B-vertex (Left) or between two A-vertices (Right).

If, for example, there is a B-vertex to the right of v (Fig. 5, Left), then this B-vertex emanates from a G-vertex $\tilde{v}$ in level $k-1$. Since $i_k(\tilde{v}) \in [0, q_k)$, the relation (13) or (14) implies that $\mathfrak{i}_k(v) \in [0, q_k)$ using $q_{k+1} > q_k$. Similarly, one shows $\mathfrak{i}_k(v) \in [0, q_k)$ if there is a B-vertex to the left of v.

Now suppose both neighbors of v are A-vertices. Enumerate the G-vertices emanating from the same A/B-vertex as v, from left to right, by $u_0, \ldots, u_M$, with $v = u_j$ for some j (Fig. 5, Right). Then either there exists a B-vertex to the left of u_0 (or symmetrically a B-vertex to the right of u_M), or u_0 is the left-most vertex in level k (symmetrically, u_M is the right-most vertex in level k). In either case we conclude from the previous considerations that $i_k(u_0), i_k(u_N) \in [0, q_k)$. Since

$$Q_k(u_j) = Q_k(u_0) + \begin{pmatrix} 0 & j \\ 0 & 0 \end{pmatrix},$$

the sequence $i_k(u_j)$ is monotone in j (either decreasing or increasing depending on the parity of k). Because both endpoints $i_k(u_0)$ and $i_k(u_N)$ lie in $[0, q_k)$, it follows that $i_k(u_j) \in [0, q_k)$ for all $0 \leq j \leq M$ and in particular for the vertex v. Therefore we have established (15).

By definition of $\mathfrak{c}_k$ in (7) and (15) we have

$$\mathfrak{c}_k(v) = \begin{cases} \mathfrak{i}_k(v) & 0 \leq \mathfrak{i}_k(v) < \frac{q_k}{2}, \\ \mathfrak{i}_k(v) - q_k & \frac{q_k}{2} \leq \mathfrak{i}_k(v) < q_k. \end{cases} \tag{16}$$

From (16) together with (13), (14), we can now show the conservation of $\mathfrak{c}_k$ along the paths γ, described in the Letter.

We treat the case of odd k (the even case follows analogously), as illustrated in Fig. 4. Suppose first that $\mathfrak{c}_k(v) < 0$. Then the path $\gamma = (v_0, v_1, \ldots)$ is defined by setting $v_0 = v$ and, at each branching, choosing the right-most descendant. Since $\mathfrak{c}_k(v) < 0$, (16) gives $\mathfrak{c}_k(v) = \mathfrak{i}_k(v) - q_k$. Applying (13) and (14) it inductively (see the red colored vertices, arranged in a zigzag pattern in Fig. 4) follows that $\mathfrak{c}_k(v) = \mathfrak{c}_{k+2m}(v_{2m})$ for all $m \in \mathbb{N}$.

Next suppose that $\mathfrak{c}_k(v) > 0$. Then the path $\eta = (u_0, u_1, \ldots)$ is defined by setting $u_0 = v$ and, at each branching, choosing the left-most descendant. Since $\mathfrak{c}_k(v) > 0$, (16) gives $\mathfrak{c}_k(v) = \mathfrak{i}_k(v)$. Applying (13) and (14) it inductively (see the blue colored vertices, arranged in a zigzag pattern in Fig. 4) follows that $\mathfrak{c}_k(v) = \mathfrak{c}_{k+2m}(u_{2m})$ for all $m \in \mathbb{N}$.

D. Spectral gaps convergence along γ

Consider an irrational α with its spectral α-tree, $\mathcal{T}_\alpha$. Let v be a G-vertex with index $\mathfrak{c}_k(v)$ and let $\gamma = (v_0, v_1, \ldots)$ be the infinite path starting at $v = v_0$, which is defined in this Letter, such that the indices along it are conserved, i.e., $\mathfrak{c}_k(v) = \mathfrak{c}_{k+2m}(v_{2m})$ for all $m \in \mathbb{N}$. For each v_{2m}, the open interval $I_m = (L_m, R_m)$ denotes the spectral gap of $\mathrm{Spec}\left(H_{\alpha_{k+2m}}\right)$ represented by v_{2m}. Our goal is to verify that these spectral gaps I_m converge to the limiting spectral gap $I = (L, R)$ in $\mathrm{Spec}\left(H_\alpha\right)$, which carries the same index $\mathfrak{c}_k(v)$.

We have two cases: either v_{2m} is the right-most vertex emanating from v_{2m-1} for all $m \in \mathbb{N}$ or it is always the left-most vertex. Without loss of generality we assume that v_{2m} is the right-most vertex for all $m \in \mathbb{N}$. We note that there is a neighboring path $\tilde{\gamma} = (w_0, w_1, \ldots)$ whose G-vertices share the same index values as the G-vertices of γ. For this path, w_0 is set to be the neighboring vertex at level $k+1$ to the right of the B-vertex emanating from v_0 (see Fig. 4 with $v_0 = v$ and $w_0 = w$). For the rest of the vertices of $\tilde{\gamma}$ we choose w_{2m} to be the left-most vertex emanating from w_{2m-1} for all $m \in \mathbb{N}$. By this construction we get that the vertex w_m is the right neighbor of the vertex v_{m+1} for all $m \in \mathbb{N}$.

Recall that the spectral gap associated with the G-vertex v_{2m} is $I_m = (L_m, R_m)$. By construction, the right endpoint $R_m \in \mathrm{Spec}\left(H_{\alpha_{k+2m}}\right)$ belongs to the spectral band associated with the B-vertex w_{2m+1}. These B-vertices correspond to spectral bands of the periodic operators, which form a decreasing nested sequence. Their intersection is a single point [29], lying in $\mathrm{Spec}\left(H_\alpha\right)$ and serving as the right endpoint R of the limiting gap I. Thus $R_m \to R$ as $m \to \infty$.

Moreover, $\mathrm{Spec}\left(H_{\alpha_{k+2m}}\right) \to \mathrm{Spec}\left(H_\alpha\right)$ as $m \to \infty$ [32], which implies that the left endpoints also converge, $L_m \to L$. Hence the gaps $I_m = (L_m, R_m)$ converge to the limiting gap $I = (L, R)$ of $\mathrm{Spec}\left(H_\alpha\right)$.

E. Negative indices versus positive indices

We comment here on the comparison between negative values of $\mathfrak{c}_k(v)$ versus positive values. For this discussion, recall the notation $\mathfrak{i}_k(v) := (-1)^k \det Q_k(v)$ (as in Sec. A and C) and the connection (16) between $i_k(v)$ and $\mathfrak{c}_k(v)$. We discuss to the particular case $i_k(v) = \frac{q_k}{2}$ for which one should determine the sign for $\mathfrak{c}_k(v) = \pm\frac{q_k}{2}$. This decision breaks the symmetry of the modulus window chosen for mod^*, i.e., whether the image of the modulus is $\left[-\frac{q_k}{2}, \frac{q_k}{2}\right)$ or $\left(-\frac{q_k}{2}, \frac{q_k}{2}\right]$. This decision was already made in (7) (see also (16)) and we justify it here.

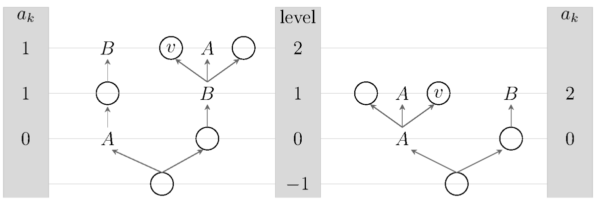

Figure 6. Two examples of spectral trees with a marked vertex v in level k which is either sandwiched between B and A vertices and k is even (Left) or v is sandwiched between A and B vertices and k is odd (Right).

As a guiding example we take $q_k = 2$. In this case, there are two spectral bands and only one bounded gap. We discuss the possible index value of that gap. To do so, consider a spectral tree $\mathcal{T}_\alpha$ with α having a continued fraction expansion starting with 2 (see Fig. 6, Right). In this tree there is a vertex v in level $k = 1$ which corresponds to the bounded gap we referred to, and indeed $q_1 = 2$. For this vertex $i_1(v) = 1 = \frac{q_1}{2}$, and we wish to explain the choice made in (7) for the modulus which gives $\mathfrak{c}_1(v) = -1$. Alternatively, $q_k = 2$ can be obtained from another spectral tree, $\mathcal{T}_\alpha$, where α has the continued fraction digits $1, 1, \ldots$ (see Fig. 6, Left). In this case there is a vertex v in level $k = 2$ for which $i_2(v) = 1 = \frac{q_2}{2}$.

In the first case above the vertex v is sandwiched between A and B vertices (in that order) and k is odd. In the second case, the vertex v is sandwiched between B and A vertices and k is even. These two cases belong to the same general class for all spectral trees: if either ***(i)*** v has A-vertex to its left and B-vertex to its right and k is odd or ***(ii)*** v has B-vertex to its left and A-vertex to its right and k is even, then $i_k(v) \geq \frac{q_k}{2}$. This justifies that the value $i_k(v) = \frac{q_k}{2}$ behaves under the modulus operation similarly to the values $i_k(v) \in (\frac{q_k}{2}, q_k)$, see (16), and hence a negative value for the index is obtained, $\mathfrak{c}_k(v) = -\frac{q_k}{2}$. We mention also the counterpart behavior: if either ***(iii)*** v has A-vertex to its left and B-vertex to its right and k is even or ***(iv)*** v has B-vertex to its left and A-vertex to its right and k is odd, then $i_k(v) < \frac{q_k}{2}$ (and $\mathfrak{c}_k(v)$ gets a positive value). The general statement above (with all of its parts (i)-(iv)) can be shown by induction, but we omit here the technical proof, and merely refer to Fig. 3, which exemplifies it.

We complement this discussion with an additional viewpoint on negative versus positive index values for $\mathfrak{c}_k(v)$. One observes (Fig. 1, Left) that the larger the absolute value of the index is, the smaller is the spectral gap and if the absolute value of two indices agree, then the one with negative index is dominant [37]. In particular, the gaps which correspond to the G-vertices whose index equals -1 are wider than those of index value 1 for all values of q_k, and hence more dominant and preferable in terms of index choice.

[1] T. Ozawa, H. M. Price, A. Amo, N. Goldman, M. Hafezi, L. Lu, M. C. Rechtsman, D. Schuster, J. Simon, O. Zilberberg, and I. Carusotto, Topological photonics, Reviews of Modern Physics **91**, 015006 (2019).

[2] E. Cherkaev, F. G. Vasquez, C. Mauck, M. Prisbrey, and B. Raeymaekers, Wave-driven assembly of quasiperiodic patterns of particles, Phys. Rev. Lett. **126**, 145501 (2021).

[3] O. Lesser and R. Lifshitz, Emergence of quasiperiodic Bloch wave functions in quasicrystals, Phys. Rev. Research **4**, 013226 (2022).

[4] J. Bellissard, K-theory of C*-algebras in solid state physics, in *Statistical Mechanics and Field Theory: Mathematical Aspects*, Lecture Notes in Physics, Vol. 257, edited by T. C. Dorlas, N. M. Hugenholtz, and M. Winnink (Springer, Berlin, Heidelberg, 1986) pp. 99–156.

[5] E. Prodan and H. Schulz-Baldes, *Bulk and Boundary Invariants for Complex Topological Insulators: From K-Theory to Physics*, Mathematical Physics Studies (Springer International Publishing, Cham, 2016).

[6] J. Kellendonk, Topological quantum numbers in quasicrystals, Israel Journal of Chemistry 10.1002/ijch.202400027 (2024), overview on the theory of topological quantum numbers in quasicrystals via non-commutative topology.

[7] N. Doll, T. Loring, and H. Schulz-Baldes, Topological indices for periodic gapped hamiltonians and fuzzy tori, Mathematical Physics, Analysis and Geometry **28**, 10.1007/s11040-025-09508-0 (2025).

[8] M. Verbin, O. Zilberberg, Y. E. Kraus, Y. Lahini, and Y. Silberberg, Observation of topological phase transitions in photonic quasicrystals, Phys. Rev. Lett. **110**, 076403 (2013).

[9] A. Dareau, E. Levy, M. B. Aguilera, R. Bouganne, E. Akkermans, F. Gerbier, and J. Beugnon, Revealing the topology of quasicrystals with a diffraction experiment, Phys. Rev. Lett. **119**, 215304 (2017).

[10] F. Baboux, E. Levy, A. Lemaître, C. Gómez, E. Galopin, L. L. Gratiet, I. Sagnes, A. Amo, J. Bloch, and E. Akkermans, Measuring topological invariants from generalized edge states in polaritonic quasicrystals, Phys. Rev. B **95**, 161114 (2017).

[11] P. Stepanov, M. Xie, T. Taniguchi, K. Watanabe, X. Lu, A. H. MacDonald, B. A. Bernevig, and D. K. Efetov, Competing zero-field chern insulators in superconducting twisted bilayer graphene, Physical Review Letters **127**, 197701 (2021).

[12] O. Zilberberg, Topology in quasicrystals, Optical Materials Express **11**, 1143 (2021).

[13] V. T. Phong and E. J. Mele, Boundary modes from periodic magnetic and pseudomagnetic fields in graphene, Phys. Rev. Lett. **128**, 176406 (2022).

[14] M. Kohmoto, L. P. Kadanoff, and C. Tang, Localization problem in one dimension: Mapping and escape, Phys. Rev. Lett. **50**, 1870 (1983).

[15] D. J. Thouless, Quantization of particle transport, Physical Review B **27**, 6083 (1983).

[16] Q. Niu and D. J. Thouless, Quantised adiabatic charge transport in the presence of substrate disorder and many-body interaction, Journal of Physics A: Mathematical and General **17**, 10.1088/0305-4470/17/12/016 (1984).

[17] G. M. Graf and J. Shapiro, The bulk–edge correspondence for disordered chiral chains, Communications in Mathematical Physics **363**, 829 (2018).

[18] D. Tanese, E. Gurevich, F. Baboux, T. Jacqmin, A. Lemaître, E. Galopin, I. Sagnes, A. Amo, J. Bloch, and E. Akkermans, Fractal energy spectrum of a polariton gas in a Fibonacci quasiperiodic potential, Phys. Rev. Lett. **112**, 146404 (2014).

[19] D. Damanik, A. Gorodetski, and W. Yessen, The Fibonacci Hamiltonian, Invent. Math. **206**, 629 (2016).

[20] D. R. Hofstadter, Energy levels and wave functions of bloch electrons in rational and irrational magnetic fields, Phys. Rev. B **14**, 2239 (1976).

[21] S. Jitomirskaya, One-dimensional quasiperiodic operators: global theory, duality, and sharp analysis of small denominators, in *Proceedings of the International Congress of Mathematicians 2022*, Vol. 2 (EMS Press, 2023) pp. 1090–1120.

[22] D. J. Thouless, M. Kohmoto, M. P. Nightingale, and M. den Nijs, Quantized hall conductance in a two-dimensional periodic potential, Phys. Rev. Lett. **49**, 405 (1982).

[23] I. Dana, Y. Avron, and J. Zak, Quantised hall conductance in a perfect crystal, Journal of Physics C: Solid State Physics **18**, L679 (1985).

[24] D. Osadchy and J. E. Avron, Hofstadter butterfly as quantum phase diagram, J. Math. Phys. **42**, 5665 (2001).

[25] J. E. Avron, D. Osadchy, and R. Seiler, A topological look at the quantum hall effect, Physics Today **56**, 38 (2003).

[26] One could replace V_α by a smooth approximation, as in [36]. This is useful for irrational frequencies, but does not fully resolve the problem for the periodic operators.

[27] J. E. Avron, O. Kenneth, and G. Yehoshua, A study of the ambiguity in the solutions to the Diophantine equation for Chern numbers, J. Phys. A **47**, 185202, 10 (2014).

[28] R. Band, S. Beckus, and R. Loewy, MFO Report: The Dry Ten Martini problem for Sturmian dynamical systems, arXiv:2309.04351 (2023).

[29] R. Band, S. Beckus, and R. Loewy, The Dry Ten Martini Problem for Sturmian Hamiltonians, arXiv:2402.16703 (2024).

[30] The description here is for $\lambda > 0$. The tree for $\lambda < 0$ is a vertical reflected image of the tree described above, see details in [29].

[31] J. Bellissard, A. Bovier, and J.-M. Ghez, Gap labelling theorems for one-dimensional discrete Schrödinger operators, Rev. Math. Phys. **4**, 1 (1992).

[32] J. Bellissard, B. Iochum, and D. Testard, Continuity properties of the electronic spectrum of 1d quasicrystals, Comm. Math. Phys. **141**, 353 (1991).

[33] R. Band, S. Beckus, B. Biber, L. Raymond, and Y. Thomas, A review of a work by Raymond: Sturmian Hamiltonians with a large coupling constant - periodic approximations and gap labels, arXiv:2409.10920 (2025), Proceedings of "CA18232: Mathematical models for interacting dynamics on networks". In press.

[34] H. Hiramoto and M. Kohmoto, New localization in a quasiperiodic system, Phys. Rev. Lett. **62**, 2714 (1989).

[35] Y. E. Kraus and O. Zilberberg, Topological equivalence between the fibonacci quasicrystal and the Harper model, Phys. Rev. Lett. **109**, 116404 (2012).

[36] J. Kellendonk and E. Prodan, Bulk-boundary correspondence for Sturmian Kohmoto-like models, Ann. Henri Poincaré **20**, 2039 (2019).

[37] This interesting observation yet awaits a rigorous explanation.